Title
Optimization of the signal-to-noise ratio of frequency-domain instrumentation for near-infrared spectro-imaging of the human brain.

Journal
Optics Express, 11(21)

ISSN
1094-4087

Authors
Toronov, Vlad
D'Amico, Enrico
Hueber, Dennis
et al.

Publication Date
2003-10-20

DOI
10.1364/oe.11.002717

Optimization of the signal-to-noise ratio of frequency-domain instrumentation for near-infrared spectro-imaging of the human brain

Vlad Toronov[1], Enrico D'Amico[2], Dennis Hueber[3], Enrico Gratton[2], Beniamino Barbieri[3], and Andrew Webb[1]

[1]*Beckman Institute for Advanced Science and Technology, University of Illinois at Urbana-Champaign, 405 N. Mathews Avenue, Urbana, IL 61801-3080*
[2]*Laboratory for Fluorescence Dynamics, Department of Physics, University of Illinois at Urbana-Champaign, 1110 W. Green Street, Urbana, IL 61801-3080*
[3]*ISS Incorporated, 1602 Newton Drive, Champaign, Il 61822*

toronov@uiuc.edu

Abstract: Frequency-domain near-infrared spectro-imaging offers significant advantages over the continuous-wave method in human brain applications. However, the drawback of existing instruments is a low signal-to-noise ratio for measured phase and modulation depth changes caused by cerebral activation. In this paper we show that in the case of the geometry specific for the activated area in the human brain, the SNR can be significantly improved by increasing the modulation frequency. We present the results of two studies: one performed experimentally using a sub-nanosecond pulsed light source and a spherical absorbing inhomogeneity immersed in a highly scattering solution, and the other performed numerically using Monte Carlo simulations of light transport in an MRI-based digital phantom of the adult human head. We show that changes caused by the absorbing inhomogeneity in both phase and modulation depth increase with frequency and reach maximum values at frequencies between 400 and 1400 MHz, depending on the particular source-detector distance. We also show that for the human head geometry an increase of the modulation frequency from 100 to 500 MHz can increase the phase SNR 2-3 times, and the modulation depth SNR up to 10 times.

OCIS codes: (170.0170) Medical optics and biotechnology; (170.5280) Photon migration; (170.5270) Photon density waves.

References and links

1. A. Villringer, J. Planck, C. Hock, L. Schleinkofer, U. Dirnagl, „Near infrared spectroscopy (NIRS): a new tool to study hemodynamic changes during activation of brain function in human adults," Neurosci. Lett. **154**, 101-104 (1993).
2. R.M. Danen, Y.Wang, X.D. Li, W.S.Thayer, A.G. Yodh., "Regional imager for low-resolution functional imaging of the brain with diffusing near-infrared light," Photochem Photobiol. **67**, 33-40 (1998).
3. C.D. Kurth and W.S. Thayer, "A multiwavelength frequency-domain near-infrared cerebral oximeters," Phys. Med. Biol. **44**, 727-740 (1999).
4. V. Toronov, A. Webb, J. H. Choi, M. Wolf, L. Safonova, U. Wolf, E. Gratton. "Study of Local Cerebral Hemodynamic Fluctuations by Simultaneous Frequency-Domain near-infrared spectroscopy and fMRI," Optics Express **9**, 417-427 (2001), http://www.opticsexpress.org/abstract.cfm?URI=OPEX-9-8-417.
5. V. Toronov , A. Webb, S. Walker, R. Gupta, J. H. Choi, E. Gratton, D. Hueber, "The Roles of Changes in Deoxyhemoglobin Concentration and Blood Volume in the fMRI BOLD Signal," Neuroimage **19**, 1521-31 (2003).
6. G. Alexandrakis, T.J. Farrell, and M. S. Patterson, "Accuracy of the diffusion approximation in determining the optical properties of a two-layer turbid medium," Appl. Opt. **37**,7401-7409(1998).

#2824 - $15.00 US Received July 31, 2003; Revised October 12, 2003

7. D. A. Boas, M. A. OLeary, B. Chance, A. G. Yodh, " Detection and characterization of optical inhomogeneities with diffuse photon density waves: a signal-to-noise analysis," Appl. Opt. **36**, 75-92 (1997)
8. I.G. Zubal, C.R. Harrell, E.O. Smith, Z. Rattner, G. Gindi, P.B.Hoffer, "Computerized 3-Dimensional Segmented Human Anatomy," Med. Phys. **21**, 299-302 (1994), http://noodle.med.yale.edu/zubal/.
9. C. Yu, C. Mu, X. Intes, B. Chance, " Signal-to-noise analysis for detection sensitivity of small absorbing heterogeneity in turbid media with single-source and dual-interfering-source," Opt. Express **9**, 212 -224 (2001), http://www.opticsexpress.org/abstract.cfm?URI=OPEX-9-4-212.
10. D.A. Boas, J. P. Culver, J. J. Stott, and A. K. Dunn, "Three dimensional Monte Carlo code for photon migration through complex heterogeneous media including the adult human head," Opt. Express **10**, 159-170 (2002), http://www.opticsexpress.org/abstract.cfm?URI=OPEX-10-3-159.
11. J. H. Choi, , M. Wolf, V. Toronov, U. Wolf, C. Polzonetti, D. Hueber, L. Safonova, R. Gupta, A. Michalos, W. Mantulin, E. Gratton, "Noninvasive determination of absolute optical properties of adult human brain: near infrared spectroscopy approach," J. Biomed. Opt. (in press)
12. M. Firbank, E. Okada, D.T. Delpy, "A theoretical study of the signal contribution of regions of the adult head to near infrared spectroscopy studies of visual evoked responses," Neuroimage **8**, 69-78 (1998).

1. Introduction

Near-infrared biomedical spectro-imaging is a rapidly developing method, which offers significant advantages such as high biochemical specificity, high temporal resolution, and relatively low cost [1]. It has been shown that a particularly advantageous technique for imaging functional cerebral activation is frequency-domain spectro-imaging [2-6], which employs near-infrared light harmonically modulated at a frequency of 100 MHz or above. The reason for such a superiority of the frequency-domain method over the continuous-wave method is that it provides much more information, which is encoded in three parameters of the photon density wave: the intensity (DC), the modulation amplitude (AC), and the phase. However, a significant limitation of the frequency-domain method is a relatively low signal-to-noise ratio (SNR) of the phase and modulation.

Most of the current frequency-domain instruments were designed roughly a decade ago and operate at relatively low modulation frequencies around 100 MHz. Such a choice was determined not only by the higher cost of higher frequency electronics, but also by the lack of evidence that higher modulation frequencies result in significant SNR improvements. For example, although some phase SNR improvement at higher frequencies can be seen in Fig. 12 (f) in Ref. [7], the authors concluded that the highest SNR for detecting absorbing inhomogeneities in the slab geometry was at zero frequency.

However, as it was shown in Ref. [6], in the case of the non-homogeneous semi-infinite medium the cw method may be unacceptably inaccurate, and only the frequency-domain method provides positive results. The goal of this paper is to examine the frequency dependence of the SNR of the frequency-domain method in the geometry of the human head. For a geometry that is specific for a particular activated area in the human brain we study the dependence on the modulation frequency and source-detector distance of the changes caused by the absorbing inhomogeneity in two parameters: the phase and the modulation depth (MD), i.e., the ratio AC/DC, of the photon density wave. We present the results of two studies: one performed experimentally using a sub-nanosecond pulsed light source and a spherical absorbing inhomogeneity immersed in a highly scattering solution, and the other performed numerically using Monte Carlo simulations of light transport in the MRI-based digital phantom of the adult human head [9] which includes not only highly scattering tissues, but also the low-scattering cerebro-spinal fluid.

We show that changes caused by the absorbing inhomogeneity, in both phase and MD increase with frequency and reach their maximum values between 400 and 1400 MHz depending on the source-detector distance. We also demonstrate that, for a typical frequency-domain instrument, the major source of the phase and modulation noise is the quantum shot noise. Under this condition, the standard deviations of both phase and modulation noise can be analytically related to the modulation frequency through their dependence on the mean modulation amplitude (AC). Using these relationships and experimental and simulated data

#2824 - $15.00 US Received July 31, 2003; Revised October 12, 2003

we show that for the human head the SNR, i.e. the ratio of the parameter change caused by the inhomogeneity to the standard deviation of the noise in this parameter, for the frequency-domain measurement can be significantly improved by increasing the modulation frequency.

2. The noise model and its validation

As discussed in [7, 9], the sources of noise in biomedical near-infrared spectro-imaging are physiological fluctuations unrelated to the changes being studied and instrumental noise. The principal instrumental noise components in the detected signal are the quantum fluctuations of the number of electrons in the detector current (caused by the combination of the quantum noise in the input light and internal fluctuations in the number of generated photoelectrons electrons), and specific noise sources in the electronic circuits, such as the thermal noise, 1/f noise, etc. In the case where the illumination is sufficiently high, the electronic noise can be neglected compared to the quantum noise.

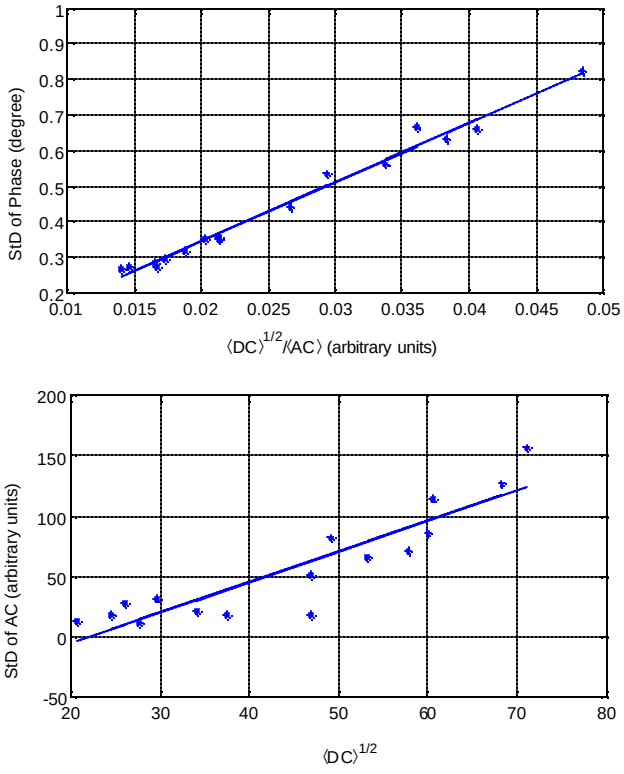

Fig. 1. Fluctuations in the frequency domain parameters acquired in-vivo using the 110 MHz ISS Oximeter. (a) Standard deviation of the phase. (b) Standard deviation of AC.

Our experience in using frequency domain instruments for biomedical spectroscopy and imaging shows that the electronic noise usually is not significant. Therefore, we limited our consideration of the instrument noise to the quantum shot noise. As we show in the Appendix (see Eqs. (17) and (18)), in this case the standard deviations of fluctuations in the modulation

#2824 - $15.00 US Received July 31, 2003; Revised October 12, 2003

amplitude and in the phase are proportional to $\sqrt{DC}$ and $\sqrt{DC}/AC$, respectively. Since the value of *AC* decreases with the frequency, the phase noise increases.

It can be also shown (see Eq. (19) in the Appendix) that the MD standard deviation is proportional to AC/DC This means that the MD noise decreases with the frequency, so that the SNR may not decrease with frequency as rapidly as the phase SNR.

Apart from the quantum noise, in-vivo measurements are affected by physiological fluctuations, in particular by hemodynamic fluctuations, respiration and vasomotion. To investigate whether the quantum noise is the dominant source of noise affecting measurements using the frequency-domain instrument, we used frequency-domain data (modulation amplitudes and phases) acquired simultaneously at a number of source-detector distances ranging from 0.5 to 4 cm using an ISS tissue Oximeter (ISS, Champaign, Il) and a probe placed on the human forehead during one of our previous studies [4]. Due to tissue attenuation, different source-detector distances gave us signals with different mean value of DC and AC. Figure (1) shows typical plots of the standard deviations in the phase and AC as functions of $\sqrt{DC}/AC$ and $\sqrt{DC}$, respectively. A typical feature illustrated in Fig 1 is that the ordinates in both plots exhibit a linear correlation with the abscissas. The linearity is particularly high in the phase plot. This indicates that, in spite of the other noise sources, quantum noise is the dominant source of noise in these *in vivo* frequency-domain measurements.

3. Experimental study of changes in frequency-domain parameters caused by an absorptive inhomogeneity immersed in a semi-infinite medium

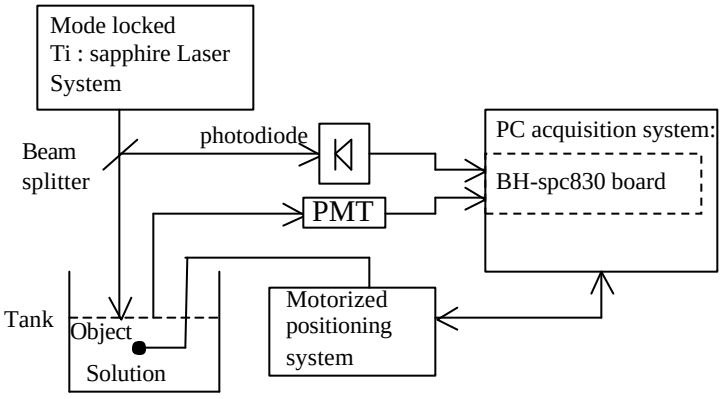

Fig. 2. Schematic of the setup for the pulsed-laser experiment

The experimental set-up (Fig. 2) consisted of a Tsunami sapphire laser system (Spectra Physics) in a femtosecond configuration, a tank containing a Liposyn (Abbott Laboratories)–black India ink solution, a photomultiplier tube (PMT), a motorized positioning system, a single photon-counting board (Beckel & Hickel model SPC-830), and a photodiode which provides the synchronization signal to the SPC-830 board.

The laser system provided a 780 nm pulsed light source at a 80 MHz repetition rate. Using a 400 μm multimode silica optical fiber the laser pulse was sent into the Liposyn India ink solution which simulated human brain in terms of the optical properties ($\mu_s' \approx 11$ cm^{-1}, $\mu_a' \approx 0.1$ cm^{-1}). The half-maximum width of the pulse at the fiber output was roughly 0.5 ns. The scattered light was collected at the surface of the medium at a variable distance from the source by means of a 3 mm fiber bundle and then sent to the PMT detector (Hammamatsu

#2824 - $15.00 US Received July 31, 2003; Revised October 12, 2003

R5600P). The acquisition system was based on the SPC-830 single photon counting board which measured the detected photon arrival times and produced a time histogram representing the averaged received pulse.

In order to model the brain activity, a 2 cm diameter spherical object with the same scattering but different absorbing properties ($\mu_s' \approx 11$ cm^{-1}, $\mu_a \approx 0.2$ cm^{-1}) was placed at 15 mm depth between the source and detector as shown in Fig. 3.

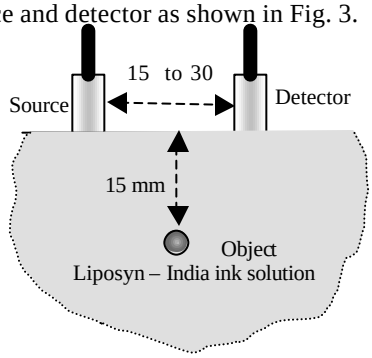

Fig. 3. Position of the object relative to the source and detector in the pulsed-laser experiment.

The distance between the source and the detector fibers was set to 15, 20, 25, or 30 mm. In order to perform measurements with and without the object, the object was moved in and out of position using a computer-controlled step-moving system which allowed movement of the object along three orthogonal axes with an accuracy of up to 5 microns/step.

In order the to avoid pulse distortions due to the pile-up effect it was important to maintain a sufficiently low light intensity at the detector input so that the photon counting rate did not exceed 100,000 photons per second. At source-detector distances of 25 and 30 mm the signal attenuation due to the medium was sufficient to fulfill this requirement, while at 15 and 20 mm distances additional attenuation by a neutral density filter was necessary. For this reason we were unable to maintain the same source power at all distances.

Each photon-counting measurement continued for 600 s. This time duration was selected to provide a sufficient ratio of the number of detected photons to the photon noise on the one hand, and to avoid significant non-stationary instabilities of the laser output occurring at large time intervals. In order to assess the signal variability each measurement was repeated four times under identical measuring conditions. The mean time shift between the averaged pulses corresponding to different measurements at the same conditions was about 15-25 ps, which corresponds to the Fourier transform phase slope of about 1-1.5°/GHz.

Figure 4(a) shows the shapes of the detected pulses: the pulse at the end of the source fiber, and pulses measured at 15 and 30 mm from the source with and without the object in place. The pulses are normalized to the maximum value of the pulse measured at the given distance without the object in place. One can see that the presence of the object decreases the pulse amplitude and shifts its maximum to an earlier time. These changes are more significant for larger source-detector distances.

In order to assess the frequency dependence of the changes caused by the object, the time-domain pulses were Fourier transformed. Since we were interested in the response to an infinitely short pulse, we divided the complex Fourier spectra corresponding to the pulses passed through the medium by the spectrum of the source pulse. Figure 4(b) shows the DC-normalized power spectra of the pulses shown in Fig. 4(a). The spectral amplitudes of pulses acquired with the object in place are normalized to the DC value of the corresponding spectra acquired without the object. Figure 4(b) demonstrates two important features. First, even at the distance of 30 mm and frequencies over 1 GHz the spectral amplitudes decrease with frequency, which indicates that the assumption that the quantum shot noise exceeds the electronic noise is valid. Second, one can see that the difference between the spectral

#2824 - $15.00 US Received July 31, 2003; Revised October 12, 2003

amplitudes with and without the object does not increase with frequency, which indicates that the signal-to-noise ratio of the AC change caused by the object can not be improved by increasing the modulation frequency.

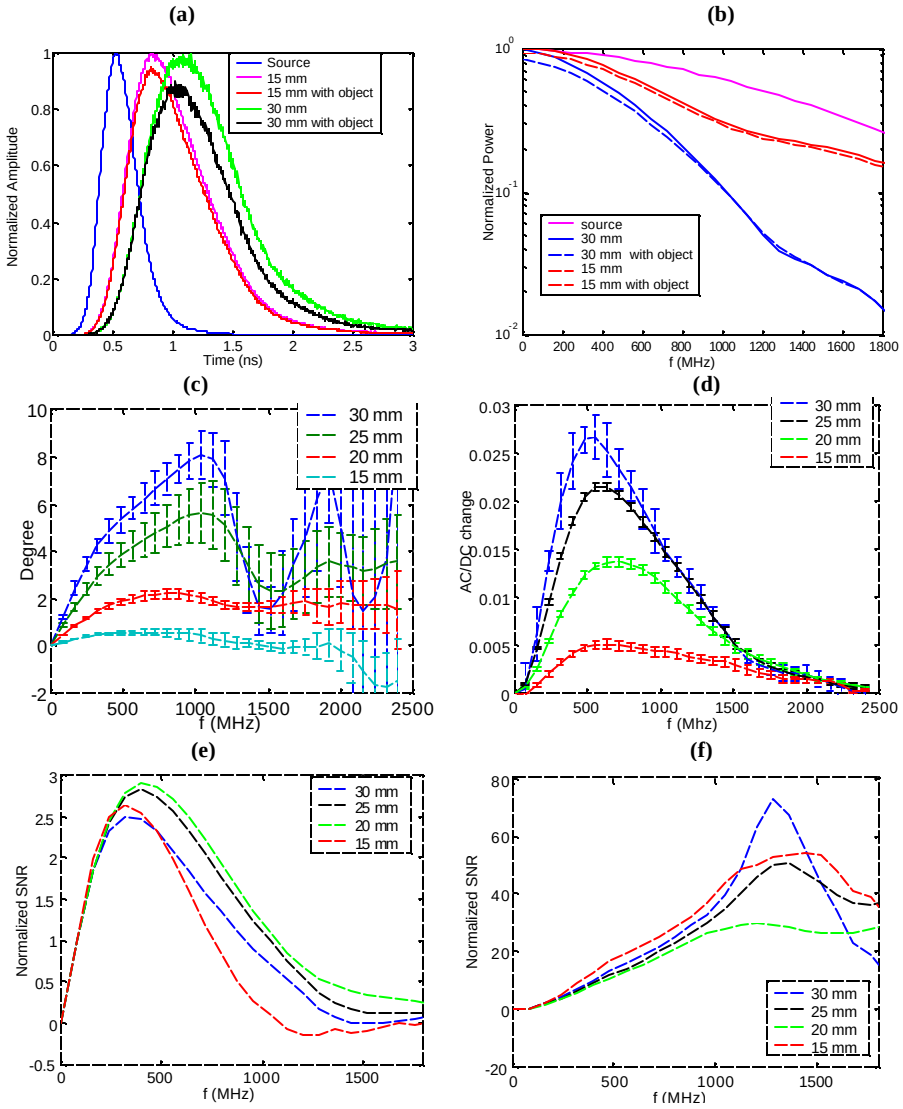

Fig. 4. Experimental data from the pulsed-laser experiment: (a) normalized source, 15 mm, and 30 mm pulses (b) Fourier power spectra of pulses shown in Fig 4(a); (c) changes in phase caused by the absorbing inhomogeneity, (d) changes in modulation depth (AC/DC ratio); (e) phase SNR as function of modulation frequency; (f) MD SNR as function of frequency. In Figs. 4(e) and (f) the SNR values are computed using the analytical noise model. Values corresponding to each curve are normalized to the value for the same curve at 100 MHz

The situation is qualitatively different in the case of changes in the phase and in the MD (see Figs. 4(c) and 4(d), respectively). Changes in these parameters increase significantly with frequency and show maxima at frequencies from 600 to 1200 MHz (depending on the source-detector distance) in case of the phase change, and from 500 to 700 MHz in case of the ratio AC/DC. The error bars in Figs. 4(c) and (d) show average errors corresponding to measurements repeated four times. In Fig. 4(c) one can see that the phase error increases with

#2824 - $15.00 US Received July 31, 2003; Revised October 12, 2003

frequency according to the model based on quantum noise. In case of the MD signal (Fig. 4(d)) the error does not increase with frequency, which also agrees with the quantum noise model. The fact that the MD error in Fig. 4(d) does not generally decrease with frequency is due to the small long-term instabilities in the laser pulse, which slightly modify its shape during different photon-counting measurements. These instabilities are specific for the pulsed laser used in this study, but not for a well designed frequency-domain instruments utilizing intensity-modulated light sources. Also, only four measurements at each condition could not provide sufficient statistical power for the direct experimental noise assessment. Therefore, to access the SNR frequency dependence (Figs. 4(e) and (f)) for the signals shown in Figs. 4(c) and (d) we used Eqs. (18) and (19) from the Appendix rather than the experimental errors.

Since the photon counting method required using additional light attenuation at smaller distances, we could not normalize the SNR obtained at different distances. Therefore, in both Figs. 4(e) and (f) all curves are normalized to the corresponding SNR values at 100 MHz. Thus, Figs. 4(e) and (f) do not compare the SNRs for signals at different distances, but rather show the SNR changes from their respective values at 100 MHz. Fig. 4(e) shows that, depending on the distance, the phase SNR reaches its maximum in the range of 300-500 MHz. In this frequency range the improvement compared to 100 MHz is quite significant (2.5-3 times). According to Fig. 4(e) the maximum improvement is reached at source-detector distances of about 20-25 mm. At smaller distances the phase signal is too small, while at a larger distance the phase noise becomes too large.

The main difference between the phase and MD SNRs is that the phase SNR peaks between 300 and 500 MHz, while the AC/DC SNR grows monotonically until about 1200 MHz. This happens because, in the case of the MD SNR, the values corresponding to the signal curves in Fig. 4(d) are divided by the AC values, which decline monotonically with frequency. It is interesting to note that in the range of 300-500 MHz where the phase SNR reaches maximum, the MD SNR at different distances increases about 5-10 times compared to its value at 100 MHz.

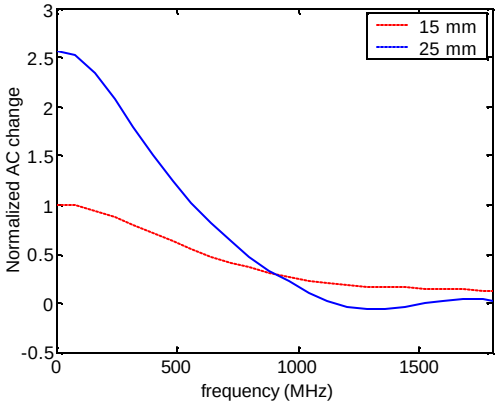

Fig. 5. Changes in AC SNR caused by the absorbing object. Data is normalized to the DC SNR at 15 mm.

It is important to compare the frequency dependence of the phase and MD SNR with the AC one. The AC SNR at 15 mm and 25 mm source-detector distance are shown in Fig. 5. Both curves are normalized to the DC SNR (zero frequency) at 15 mm. One can see that at 500 MHz both distances the signals (and the SNRs) decrease by about 50 % of the 100 MHz value. This decrease is less than the maximal phase SNR improvement and significantly less than the MD SNR improvement at 500 MHz.

#2824 - $15.00 US Received July 31, 2003; Revised October 12, 2003

4. Monte Carlo simulations of changes in phase and modulation depth caused by cerebral activation

We used the Monte Carlo code described in Ref. [10]. which models propagation of light beams ("photons") in a volume specified as a collection of voxels with specific optical properties. We derived our digital phantom of the adult human head (see Fig. 6) from the high-resolution, MRI-based, segmented, computerized head phantom [8].

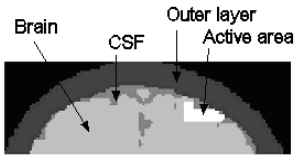

Fig. 6. MRI-based digital phantom of the adult head used in Monte Carlo simulations

The size of each voxel was 1x1x1 mm. Although the original phantom included more than 100 tissues, we simplified it by unifying various tissues into four layers: the external layer (scalp and skull), the cerebro-spinal fluid (CSF), the non-activated brain, and the activated brain (see Fig. 6). The absorption coefficients of these layers were 0.1 cm^{-1}, 0.01 cm^{-1}, 0.1 cm^{-1}, and 0.13-0.26 cm^{-1} (since no absolute values for the optical properties of the activated brain tissue have yet been published, in our simulations we used various values of μ_a in the range 0.13-0.26 cm^{-1}.), respectively. The reduced scattering coefficients were 10 cm^{-1}, 1.0 cm^{-1}, 10 cm^{-1}, and 10 cm^{-1}, respectively. The values of absorption and reduced scattering coefficients for the outer layer and the brain correspond approximately to those we obtained in our experimental study [11]. The values of the optical properties for the low-scattering and low-absorbing CSF layer (μ_a=0.01 cm^{-1} and μ'_s=1 cm^{-1}) were taken from the literature [10]. The activated area of diameter about 1.5 cm was selected in the primary motor cortex (see Fig. 6).

In the simulations the light source was positioned on the surface of the phantom above the activated area. The detectors were positioned at various surface locations at distances of 15, 20, 30, and 40 mm from the source. We recorded changes in the light energy fluence during an interval of 6-8 ns with a temporal resolution of 200 ps. The code stored the travel history and the energy of the light rays acquired by the detectors. In each simulation 10^8 rays were propagated. These data were used to calculate the phase and the MD of the detected photon-density waves with and without activation, and the SNR for the changes in these parameters caused by activation (see [10] for details).

Figures 7(a-d) show the simulated changes in the phase and MD, and the corresponding SNRs as functions of the modulation frequency. As in Figs. 4 (e) and (f), the curves in Figs. 7(c) and (d) compare the SNR for each distance with their respective values at 100 MHz. One can see that the behavior of the curves in all Figs. 7(a-d) is quantitatively very similar to the corresponding curves obtained experimentally using the pulsed laser (see Figs. 4(c-f)). Similar to Figs. 4(e) and (f), Figs. 7(c) and (d) demonstrate significant SNR increase at higher frequencies. An interesting feature seen in Fig. 7 (c) is that at frequencies higher than 300 MHz the SNR increase with frequency at the 35 mm source-detector distance is smaller than at 30 mm. This phase SNR saturation effect at larger source-detector distances can be also seen in the experimental data shown in Fig. 4(e). Saturation occurs due to the higher phase noise at larger distances. In Fig. 7 (d) one can see that at the source-detector distance about 30 mm the increase of the MD SNR also reaches saturations. Unlike the phase SNR, this happens not due to the higher noise, but because the MD signals are smaller at distances larger than 30 mm (see Fig. 7(b)).

#2824 - $15.00 US Received July 31, 2003; Revised October 12, 2003

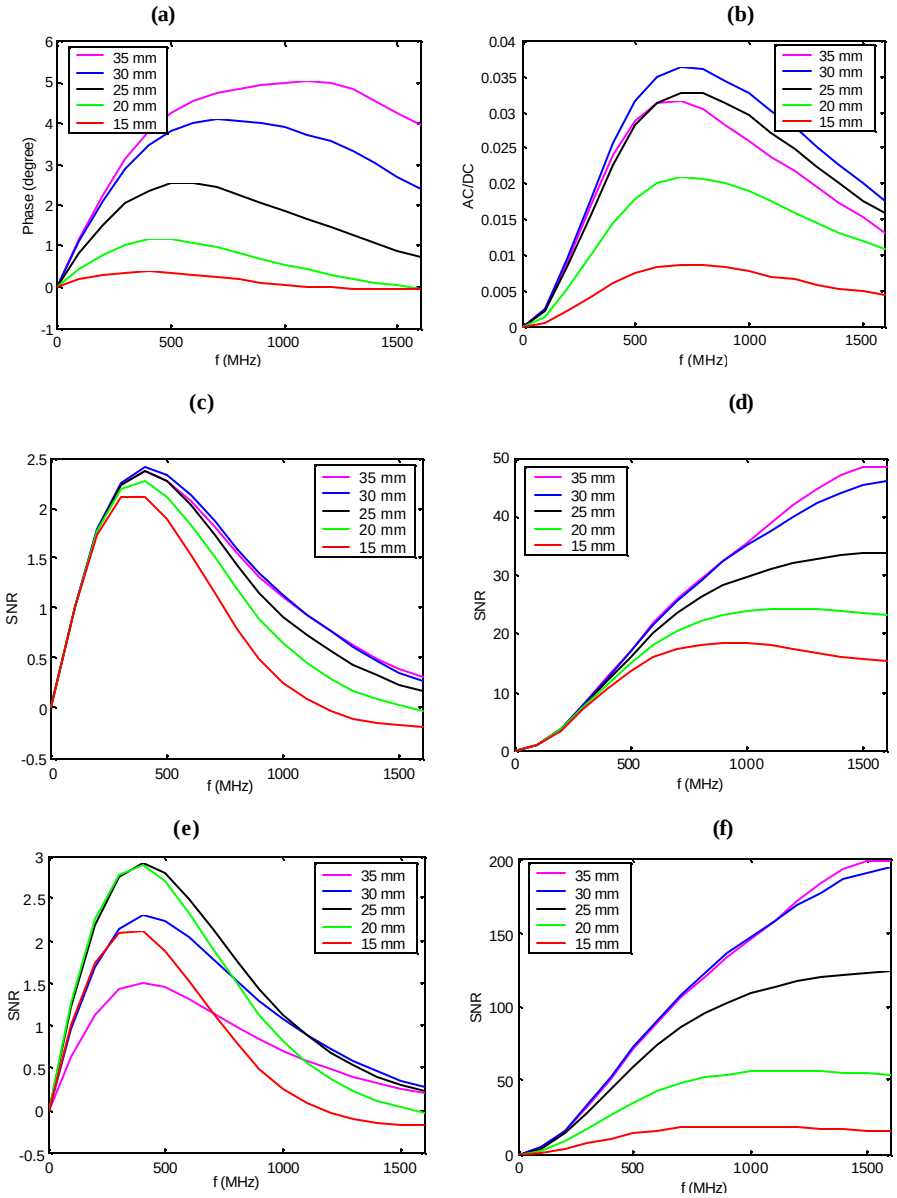

Fig. 7. Monte Carlo simulated Data:): (a) changes in phase caused by the absorbing inhomogeneity, (b) changes in modulation depth; (c) phase SNR as function of modulation frequency normalized to the 100 MHz value for the same distance; (d) MD SNR as function of frequency normalized to the 100 MHz value for the same distance; (e) phase SNR as function of modulation frequency normalized to the 100 MHz value for the 15 mm curve; (f) MD SNR as function of frequency normalized to the 100 MHz value for the 15 mm curve.

In Figs. 7(e) and (f) the SNR curves for simulated phase and MD changes are normalized to the values corresponding to 100 MHz and a source-detector distance of 15 mm. Thus, these figures compare the SNR behavior at different frequencies and at different distances with that at 100 MHz and 15 mm. In Fig. 7(e) one can see that the phase SNR significantly decreases at distances larger than 25 mm. Fig. 7(f) shows that, although at larger distances and higher frequencies the MD SNR very significantly exceeds its value at 15 mm and 100 MHz, the

#2824 - $15.00 US Received July 31, 2003; Revised October 12, 2003

curves for 30 and 35 mm are very similar. These features indicate that while an increase in the modulation frequency leads to a significant SNR improvement, the optimal source-detector distance does not exceed 30 mm.

5. Discussion

For the geometry of the human head we have found, both experimentally and using the Monte-Carlo simulation, that the changes caused by an absorbing inhomogeneity to the modulation depth and phase of the photon density wave exhibit a non-monotonics dependence on the modulation frequency. The change in phase reaches maximum between 400 and 1400 MHz, and the MD change achieves its maximum value in the 500-600 MHz frequency range depending on the source-detector distance. Such a resonance-like dependence of signals caused by inhomogeneity is specific for the situation when a relatively small object is immersed in a semi-infinite medium at the depth about 15 mm. Such a non-monotonic behavior of optical signals was not found in the case of the slab geometry [7].

We have experimentally demonstrated that for a typical frequency-domain instrument, such as the ISS Oximeter, the noise in the AC and phase data acquired *in vivo* corresponds to the quantum shot noise model, for which the dependence of the phase and MD noise on the frequency can be obtained analytically.

The most important result of our study is that for the specified geometry the SNR of the frequency-domain instrument can be significantly improved by increasing the modulation frequency. The phase SNR can be increased 2-3 times compared to the value at 100 MHz, which is comparable with the improvement demonstrated for the slab geometry in [7]. The MD SNR can be theoretically increased more than 10 times, provided that the modulation frequency is sufficiently high. Current electronics allows modulation of light sources at frequencies up to 400-500 MHz with a modulation depth of more than 30 %. Therefore, the discussed significant SNR improvement is now achievable in practice.

The amplitude SNR decreases with the frequency slower than the phase and the modulation SNR increase. Also, in our instrument the amplitude SNR at 100 MHz is quite high, and, besides, can be improved by increasing the DC. Therefore at frequencies below 500 Hz the increase in the phase SNR will not be obtained for the price of unacceptably low amplitude SNR.

We have also found that for the specified geometry both phase and MD SNR are optimized at source-detector distances of about 20-30 mm. Increasing source-detector distances to greater than 30 mm causes the phase SNR to decrease due to the higher noise, and the lower signal. This conclusion agrees with the one of [12]. However, unlike Firbank et al [12], we did not observe saturation of the phase change at larger distances, and the SNR decrease we found is due to the higher noise.

The results of both studies are close not only qualitatively, but also quantitatively. This indicates that the demonstrated influence of the modulation frequency and source-detector distance on the phase and MD SNR is related to the common features of both models, such as the geometry and the values of the optical properties of layers, which play the most important role in the light transport. Thus we should conclude that including the CSF layer intohe digital model does not cause significant effect on the phase and modulation depth.

The superiority of the frequency-domain method over the cw one has been demonstrated in a number of studies [2-6], and now is accepted by the near-infrared community. The most fundamental advantage of the frequency-domain method over the cw one is the increased amount of quantitative information about the optical properties of the medium encoded into the phase and the amplitude data. This information increase is, first, due to the different influence of the absorption and scattering on the DC, AC, and on the phase, and, second, due to the differences in the volumetric photon measurement density functions corresponding to the amplitude and the phase. Therefore, measurements of various parameters, such as the phase and the MD should increase the resolving capability of the method. For example, in the case of a homogeneous medium the frequency-domain method provides a very accurate separation of the absorptive and scattering properties [5]. For the non-homogeneous layered

#2824 - $15.00 US Received July 31, 2003; Revised October 12, 2003

semi-infinite medium it was shown in [6] that the cw method does not work, and only using both amplitude and phase measurements one can correctly reconstruct the optical properties of the internal layers. These examples suggest that the improvement of the phase and MD SNR should also improve the overall accuracy of the reconstruction of the tissue optical properties. To further investigate this issue we plan to perform the frequency-domain imaging experiments at different modulation frequencies.

6. Conclusion

In phantom experiments with sub-nanosecond light pulses, and using numerical Monte-Carlo simulations we have found that changes in the phase and modulation depth of a photon-density wave caused by local functional activation in human brain exhibit non-monotonic dependence on frequency, with a maximum value corresponding to frequencies between 400 and 1400 MHz depending on the source-detector distance. We have experimentally demonstrated that for a typical frequency-domain instrument the noise in the AC and phase data acquired *in vivo* corresponds to the quantum shot noise model. We have shown that the SNR for these changes can be very significantly improved compared to its value at 100 MHz by increasing the modulation frequency to 400-500 MHz. The source-detector distance which optimizes the SNR for both phase and modulation depth signals is about 20-25 mm.

Acknowledgment

This work was supported by the NIH SBIR grant no. NS 38378-03

Appendix

In order to estimate the noise in the phase and MD consider the transformations of the signal and noise in a frequency domain instrument. The light intensity at the detector input is

$$I(t) = a\cos(wt + f) + b \tag{1},$$

where a, b, w and f are the modulation amplitude, the intensity, the modulation frequency, and the phase of the photon density wave, respectively The detector anode current is proportional to the number of photo-electrons N_{pe} induced by light per unit of time:

$$i(t) = q\Delta f g(t) N_{pe} \tag{2}$$

where q is the electron charge, Df is the bandwidth, and $g(t)$ is the gain. Alternatively, $i(t)$ can be represented as a sum of the average value and the fluctuation

$$i(t) = \langle i(t) \rangle + x(t), \tag{3}$$

where $\langle\ \rangle$ denotes an ensemble average, and $x(t)$ is a non-stationary random process with the zero average. The ensemble average value $\langle i(t) \rangle$ at each moment of time can be obtained by averaging the right hand side of Eq. (2), which is proportional to $\langle N_{pe} \rangle$ (assuming that the gain noise is small compared to the variation in the number of photoelectrons). Since

$$\langle N_{pe}(t) \rangle = \frac{hS}{hn\Delta f} I(t), \tag{4}$$

where h and S are the quantum efficiency and the detecting area of the detector, and n is the frequency of light, $\langle i(t) \rangle$ can be written as

#2824 - $15.00 US Received July 31, 2003; Revised October 12, 2003

$$\langle i(t)\rangle = G(t)I(t), \tag{5}$$

where $G(t) = \frac{qhS}{hn} g(t)$. The gain of the detector is modulated at a frequency $w' = w + \Omega$, where the cross-correlation frequency W is very small compared to w: $g(t) = g_0(1 + m\cos(w't + f))$, $m \le 1$. Therefore, Eq. (5) can be rewritten as

$$\langle i(t)\rangle = (A\cos(wt + f) + B)(1 + m\cos(w't)), \tag{6}$$

where *A* and *B* are the constants proportional to *a* and *b*, respectively.The cross-correlation waveforms of the detector signal (i.e., waveforms of period T=2π/Ω) are then Fourier transformed to obtain the complex value *X*:

$$X = \frac{4}{T}\int_{-T/2}^{T/2} i(t)e^{-i\Omega t}dt = Ae^{if} + y\ , \tag{7}$$

where $y = \frac{4}{T}\int_{-T/2}^{T/2} x(t)e^{-i\Omega t}dt$ is the complex random error. The *AC* and phase are then obtained as

$AC = \sqrt{(X')^2 + (X'')^2}$, $\Phi = \arctan(\frac{X''}{X'})$ with mean values equal to *A* and *f*, respectively. The variances in the corresponding errors are

$$s_{AC}^2 = \cos^2(f)\langle y'^2\rangle + \sin^2(f)\langle y''^2\rangle + 2\sin(2f)\langle y'y''\rangle \tag{8}$$

and

$$s_{\Phi}^2 = \frac{\sin^2(f)\langle y'^2\rangle + \cos^2(f)\langle y''^2\rangle - 2\sin(2f)\langle y'y''\rangle}{A^2}, \tag{9}$$

respectively. The DC value is obtained using the Fourier transform at zero frequency, i.e.

$$DC = \frac{4}{T}\int_{-T/2}^{T/2} i(t)dt = \langle DC\rangle + z\ , \tag{10}$$

where $\langle DC\rangle = 4B$, and z is the random DC error equal to

$$\frac{4}{T}\int_{-T/2}^{T/2} x(t)dt\ . \tag{11}$$

To estimate the error in AC, DC, and phase one should consider the statistical properties of the random process $x(t)$. We assume that the gain noise is small, and the light intensity is high enough to neglect the thermal noise and other sources of electronic noise. Then, the only

#2824 - $15.00 US Received July 31, 2003; Revised October 12, 2003

source of noise in *i(t)* is the fluctuation of the number of photoelectrons, i.e., the shot noise, and the cross-correlation function for $x(t)$ is

$$\langle x(t')x(t'')\rangle = s_i^2(t')d(t'-t''), \tag{12}$$

where $s_i^2(t')$ is the variance. Assuming that the mean squared fluctuation in the number of photoelectrons is equal to $\langle N_{pe}\rangle$, from Eq. (2) one can derive

$$s_i^2(t) = q\Delta f g(t)\langle i(t)\rangle = a(A\cos(wt+f)+B)(1+m\cos(w't))^2, \tag{13}$$

where a is a constant. Using Eqs. (11), (12) and (13) one obtains

$$\langle y'^2\rangle = \langle y''^2\rangle = a\frac{4(2+m)}{T}B = a\frac{(2+m)}{T}\langle DC\rangle, \tag{14}$$

$$\langle y'y''\rangle = 0, \tag{15}$$

and

$$s_{DC} = \sqrt{\langle z^2\rangle} = g\sqrt{\langle DC\rangle}, \tag{16}$$

where $g = \sqrt{2a(2+m^2)/T}$. By substituting (14) and (15) into (8) and (9) we arrive at:

$$s_{AC} = b\sqrt{\langle DC\rangle}, \tag{17}$$

and

$$s_\Phi = \frac{b\sqrt{\langle DC\rangle}}{\langle AC\rangle}, \tag{18}$$

where $b = \sqrt{2a(2+m)/T}$.

In practice the detector signal is digitized with a sampling rate which is a multiple of the cross-correlation frequency *W*, and the integrals in Eqs. (7), (10), and (11) are approximated by finite fast Fourier transforms. However, one can show that Eqs. (14)-(18) are valid both for both discrete and continuous Fourier transforms. It is important to note that, as follows from Eqs. (17) and (18), s_{AC} does not depend on the modulation frequency *w*, and s_Φ depends on *w* through $\langle AC\rangle$ in the denominator.

By propagating the noise through the ratio $\langle AC\rangle/\langle DC\rangle$ one can show that the corresponding standard deviation is

$$s_{\langle AC\rangle/\langle DC\rangle} = \langle AC\rangle/\langle DC\rangle\sqrt{s_{AC}^2 + s_{DC}^2/\langle DC\rangle^2}, \tag{19}$$

Equation (19) shows that, since s_{AC}^2 and s_{DC}^2 do not depend on the modulation frequency, the dependence of the MD noise on frequency is given by the ratio of $\langle AC\rangle/\langle DC\rangle$.

#2824 - $15.00 US Received July 31, 2003; Revised October 12, 2003